

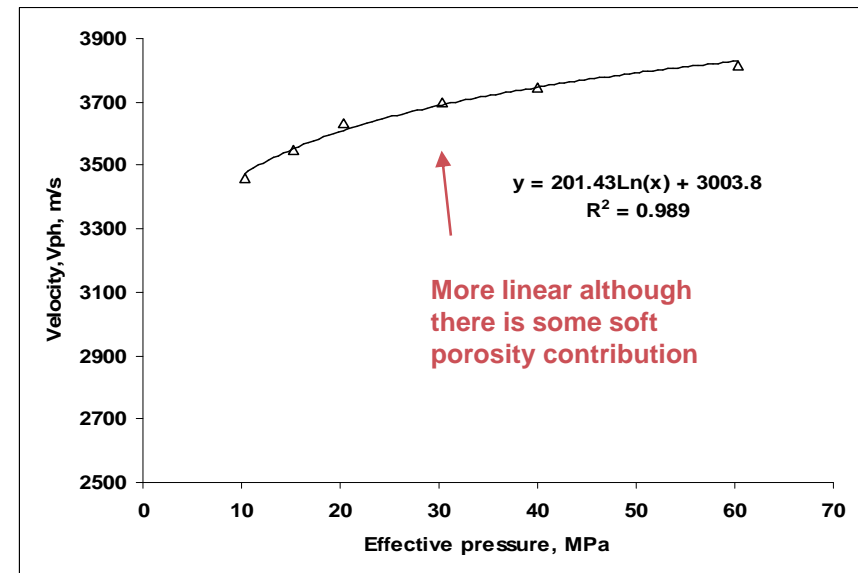
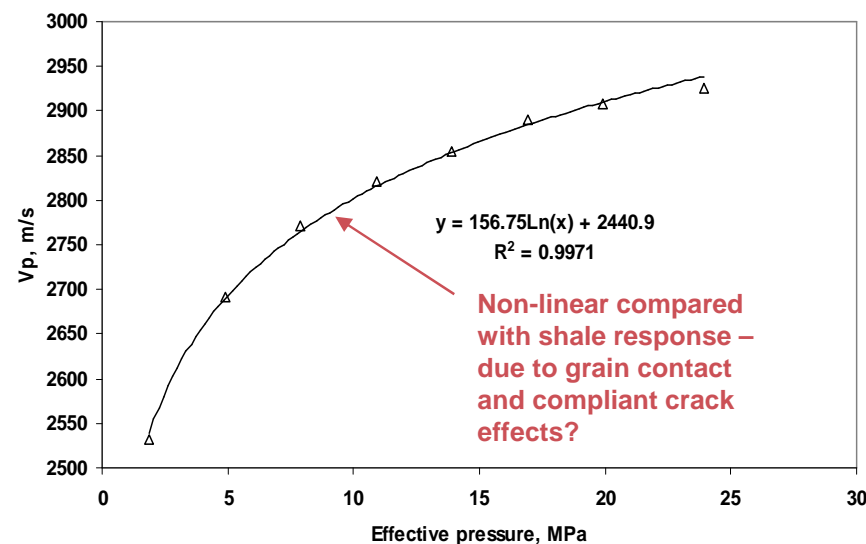
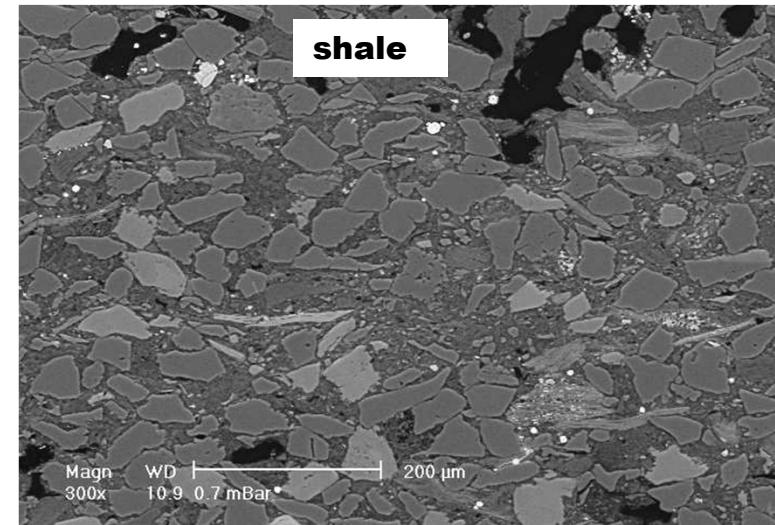
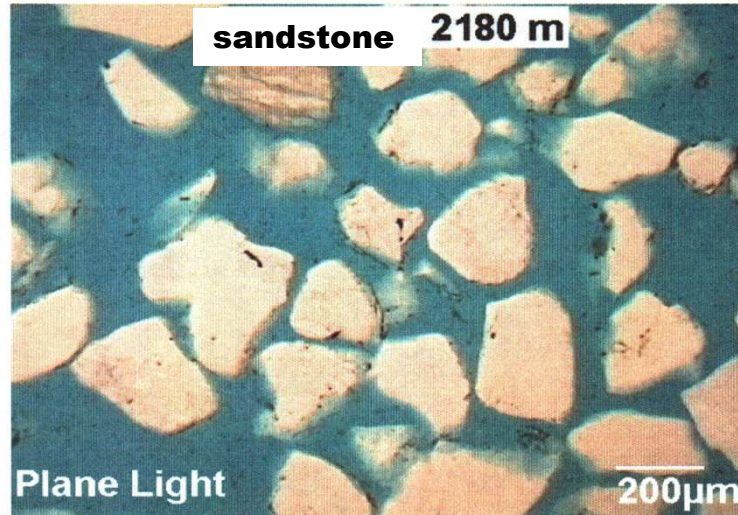
[www.csiro.au](http://www.csiro.au)

## The Visco-elastic Response of Shale at Ultrasonic Frequencies

A.F. Siggins, R. Holt and D.N. Dewhurst  
9<sup>th</sup> Euro Rock Mechanics Conference , 17<sup>th</sup> – 21<sup>st</sup> October,  
Trondheim 2011

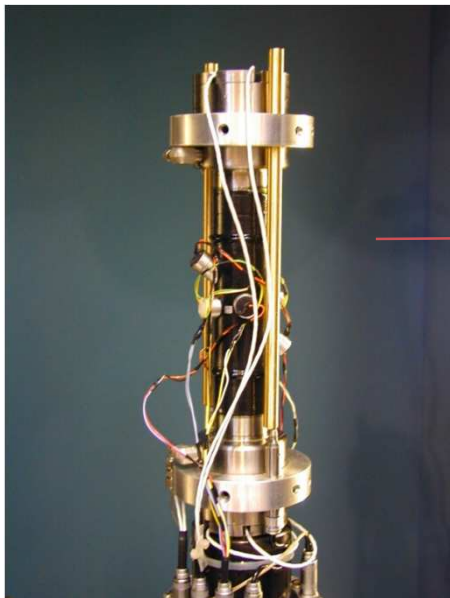


# Experimental observations - velocity



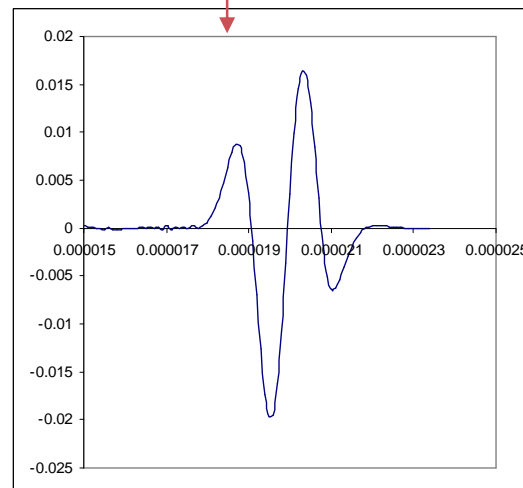
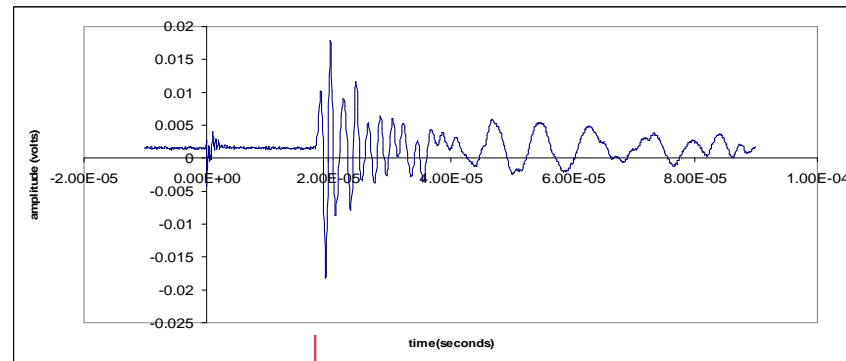
# Experimental

## Digital recording of transmitted pulses



**Ultrasonic array  
(inside pressure cell)**

### Transmitted P-wave



**Windowed P-wavelet**

# The spectral ratio method

$$A(f) = A_0 G(x) e^{-\alpha(f)x} e^{-2\pi i f (t-x/V)}$$

If a pulse is transmitted through the sample and also through a low loss reference material such as Aluminium ( $1/Q_{ref} \cong 10^{-5}$ ) then taking the natural log of the spectral ratio:

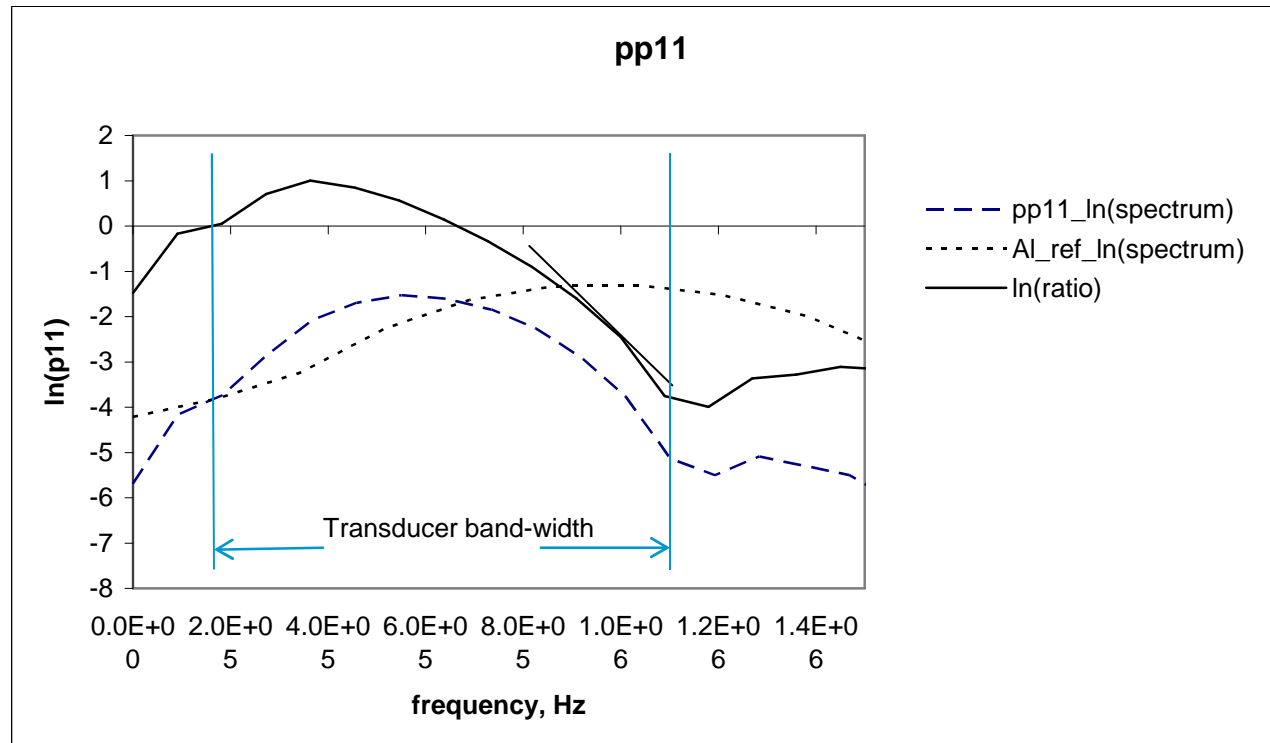
$$\ln\left(\frac{A}{A_{ref}}\right) = \ln\left(\frac{G}{G_{ref}}\right) - \frac{\pi f x}{V_p Q(f)} + \text{gain}_{-const}$$

Differentiating with respect to frequency

$$\frac{\partial \ln(A/A_{ref})}{\partial f} = -\frac{\pi x}{V_p} \left( \frac{1}{Q(f)} - \frac{f}{Q(f)^2} \frac{\partial Q(f)}{\partial f} \right)$$

If  $Q(f) \gg 1$  and the variation of velocity with frequency is mild, the derivative of the log of the normalised spectrum with frequency is proportional to attenuation,  $1/Q(f)$  to a first order approximation.

# The spectral ratio method

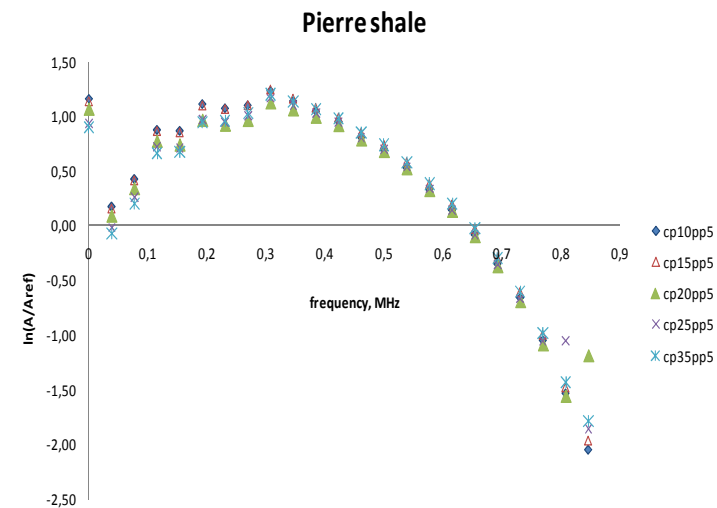
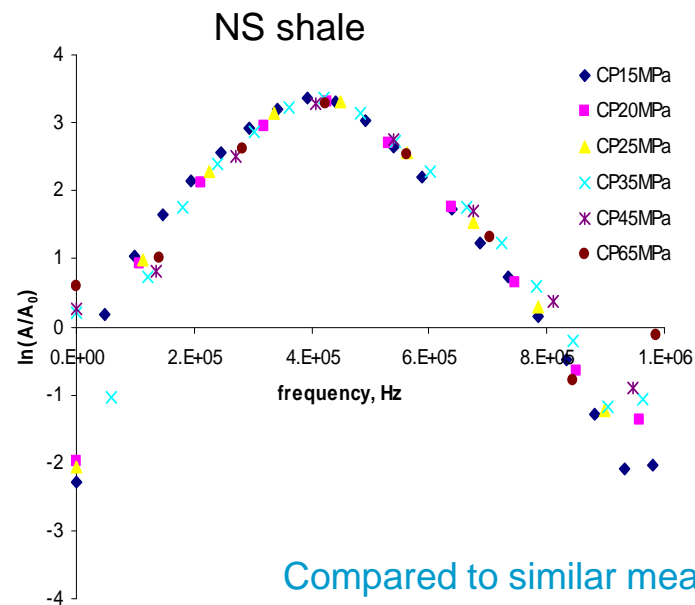


The traditional method for determining a value of attenuation,  $1/Q$  is to measure the gradient of the spectral ratio tail. However, some of the variation of  $1/Q$  with frequency is available here – at least over the transducer bandwidth.



# Experimental results for saturated NS and Pierre shales

## Spectral ratio plots



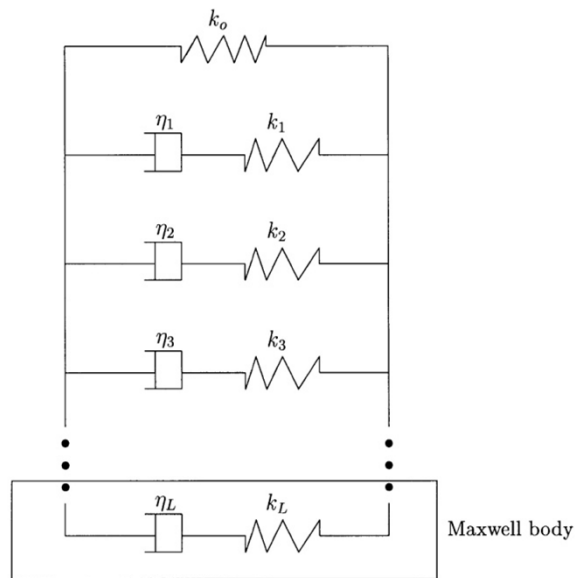
Compared to similar measurements on saturated sandstone, the spectral ratio response of these shales was relatively insensitive to effective pressure.

For the North Sea shale, confining pressure,  $P_c$  varied from 15 MPa to 65 MPa. Pore pressure,  $P_p$  was held constant at 5 MPa. With the Pierre shale,  $P_c$  varied from 10 MPa to 35 MPa with  $P_p$  constant at 5 MPa.  $P_p$  was increased step wise to 30 MPa at the end of the test sequence.

# Model fits to experiment

The generalised standard linear solid, GSLS:

(Spring-dashpot, SLS, models have been applied to poroelastic wave propagation by Carcione, 1998, Lui et al., 2010.)

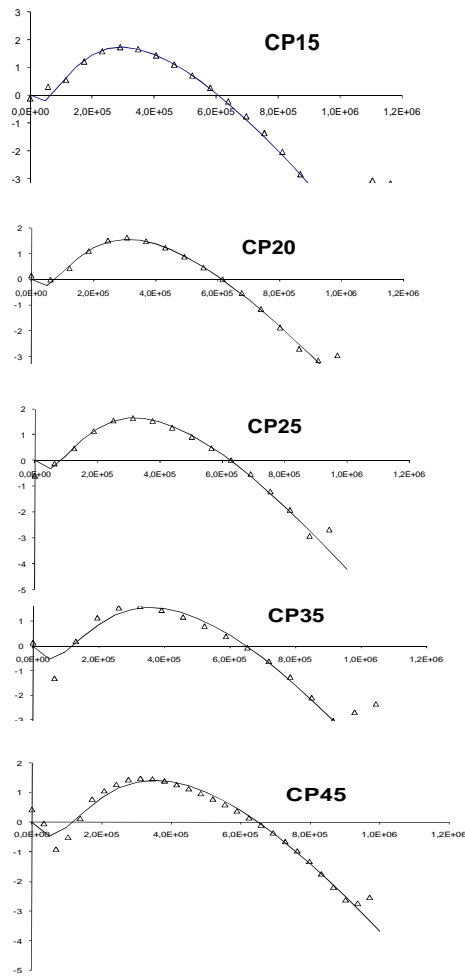


$$M(\omega) = k_0 \left\{ 1 - L + \sum_{l=1}^L \frac{1 + i\omega\tau_{\epsilon l}}{1 + i\omega\tau_{\sigma l}} \right\}$$

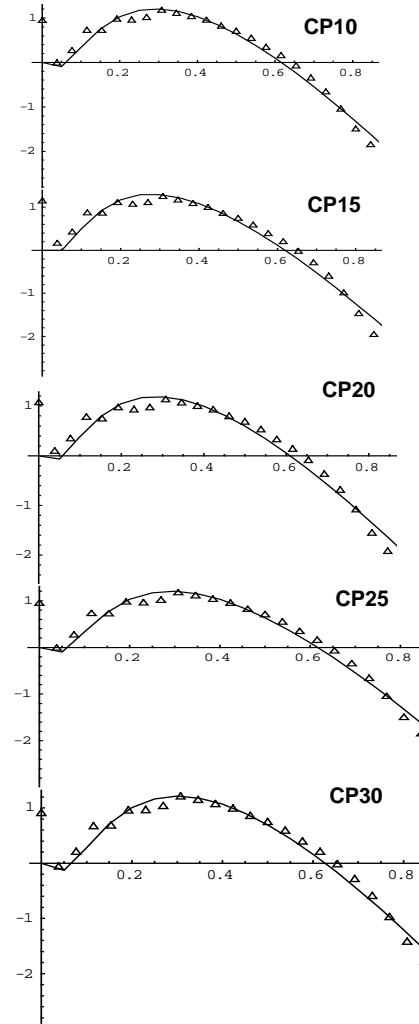
$$Q(\omega) = \frac{1 + \sum_l \frac{\omega^2 \tau_{\sigma l}^2}{1 + \omega^2 \tau_{\sigma l}^2} \tau}{\sum_l \frac{\omega \tau_{\sigma l}}{1 + \omega^2 \tau_{\sigma l}^2} \tau}$$

$1/Q(\omega)$  and a function defined by  $\int_0^{\omega} (C + \frac{1}{Q(\omega)}) d\omega$  was fitted to the expt. data.

# Integrated GSLs curve-fits as cell pressure varied



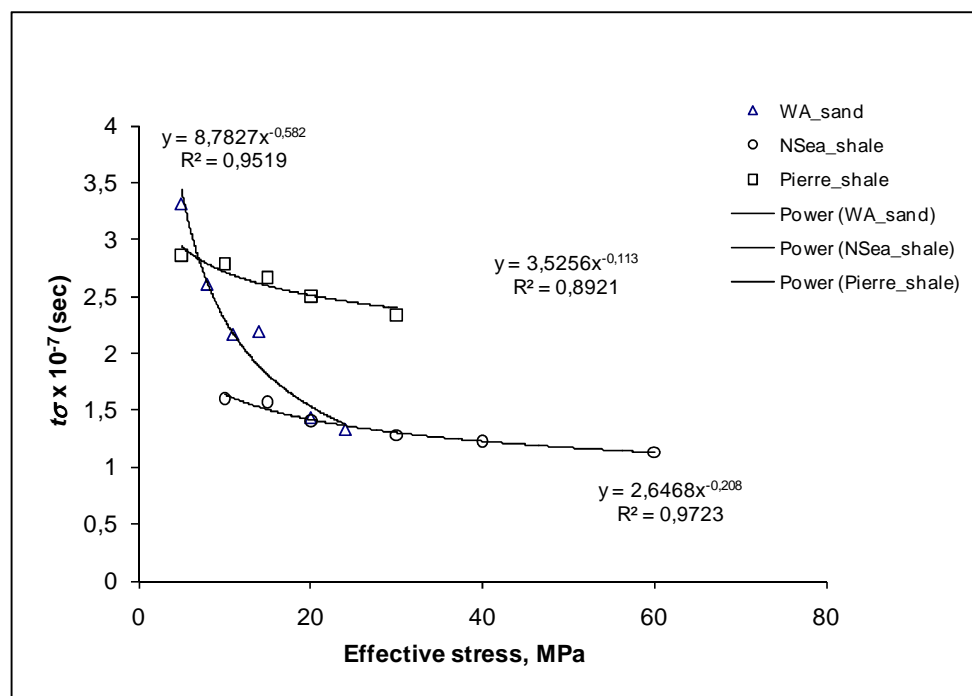
Norwegian Sea shale



Pierre shale



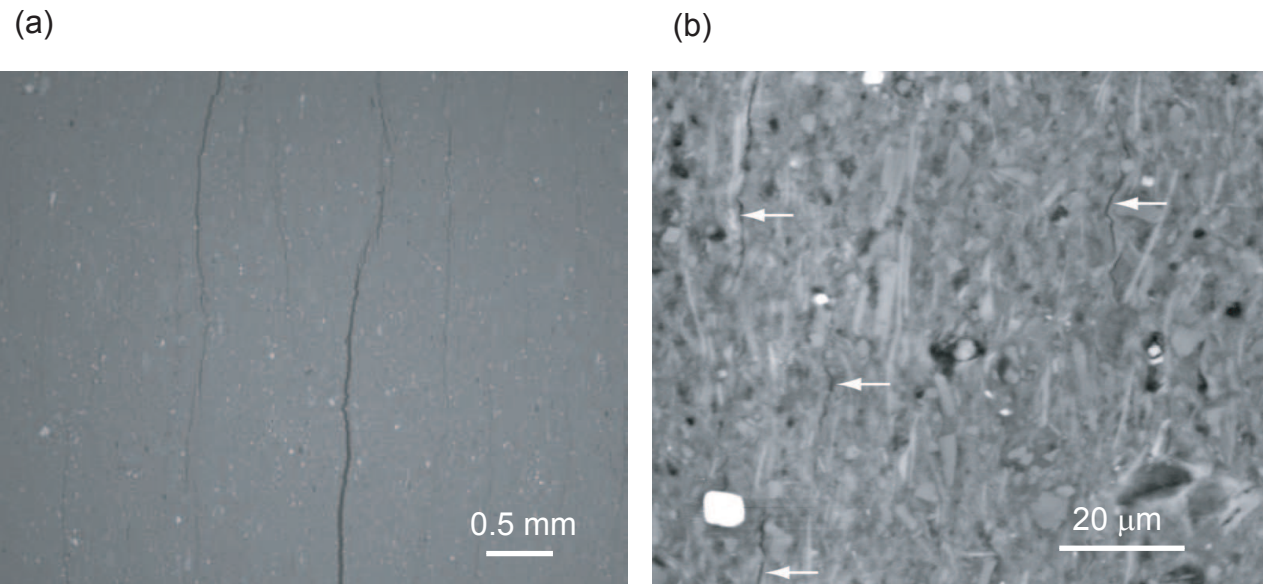
# Results of the GSLS fits to the shale data



Fitting the GSLS model to the shale experimental data yields two time constants,  $\tau_\sigma$  and  $\tau_\varepsilon$ . The variation of  $\tau_\sigma$  with effective pressure was from  $2.86 \cdot 10^{-7}$  s to  $2.34 \cdot 10^{-7}$  s, for the Pierre shale;  $1.6 \cdot 10^{-7}$  s to  $1.13 \cdot 10^{-7}$  s for the Norwegian Sea shale, both with a constant pore pressure of 5 MPa.

# Shale microstructures and soft porosity

Do shales have compliant, high aspect ratio cracks in the microstructure contributing to anisotropy and soft porosity?



Microscope images of shales often show the presence of soft porosity (a) Muderong Shale with fractures, (b) Officer Basin shale with thin microfractures (arrows). The elastic properties of shales in general show a stronger variation with pressure than implied by the total porosity change, suggesting a causal relationship with the closure of highly compliant cracks. These cracks may occupy a very small fraction of the overall pore space, but have a disproportionate effect on elastic properties of rocks due to their very high aspect ratio – adapted from Pervukhina et al., 2008.

# Velocity-effective stress implications

- Confining pressure changes in sandstones and shales result in changes in bulk modulus,  $K_b$ , mainly via collapse of soft porosity. In shales these changes are less than those observed in sandstones.
- Elastic moduli are also frequency dependent – higher moduli at high frequencies.
- In anisotropic materials like shales the elastic parameters are stress-path dependent. This leads to anisotropy changes with stress.
- Collapse of soft porosity linked to effective stress change and therefore velocity may be associated with dynamic fluid pressure changes in saturated shales. Fluid in micro cracks may play a role.
- There will be time constants associated with these pressure changes
- A Debye type frequency response can be assumed.

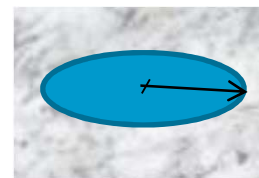
# The role of cracks in shale microstructures

The  $D$  parameter is a dimensionless parameter introduced by Budiansky and O'Connell, 1976 to describe the change of stiffness of a cracked solid when fluid is introduced to the cracks .

$$D = \frac{\xi}{\xi + 1}$$

where

$$\xi = \frac{3(1-2\nu)K_b v_c}{2f(\nu)K_f a^3}$$



crack radius,  $a$   
crack volume,  $v_c$

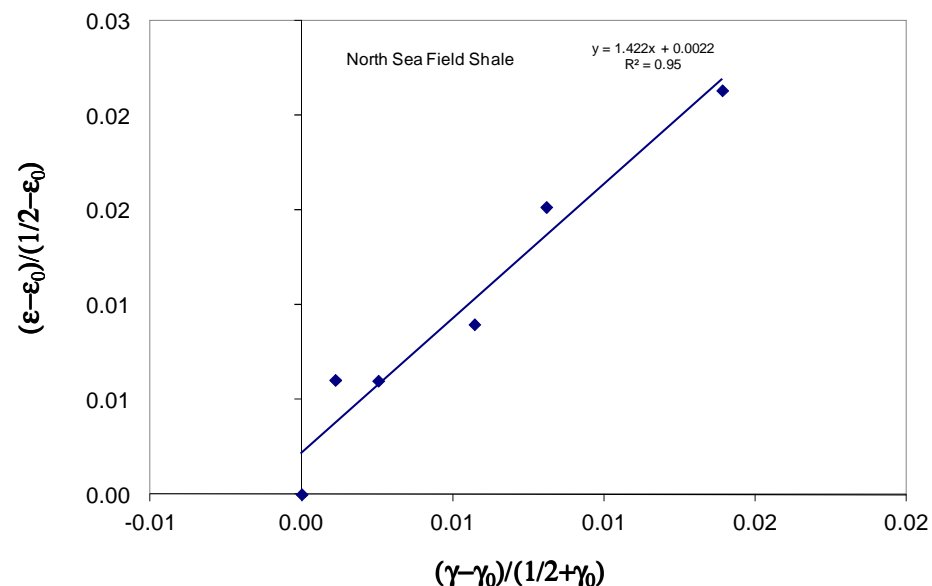
For anisotropic rock, Fjær 2006, and Holt 2009 derive an expression for  $D$  in terms of the change in Thomsen parameters,  $\varepsilon$  and  $\gamma$ ,

$$D = \frac{1-\nu}{2-\nu} \frac{\left( \frac{\varepsilon - \varepsilon_0}{1/2 + \varepsilon_0} \right)}{\left( \frac{\gamma - \gamma_0}{1/2 + \gamma_0} \right)}$$

$\nu$  is the Poisson's ratio of the fluid saturated solid.

Consequently,  $D$  is proportional to the gradient of the p-wave anisotropy versus s-wave anisotropy.

# Time constant implications

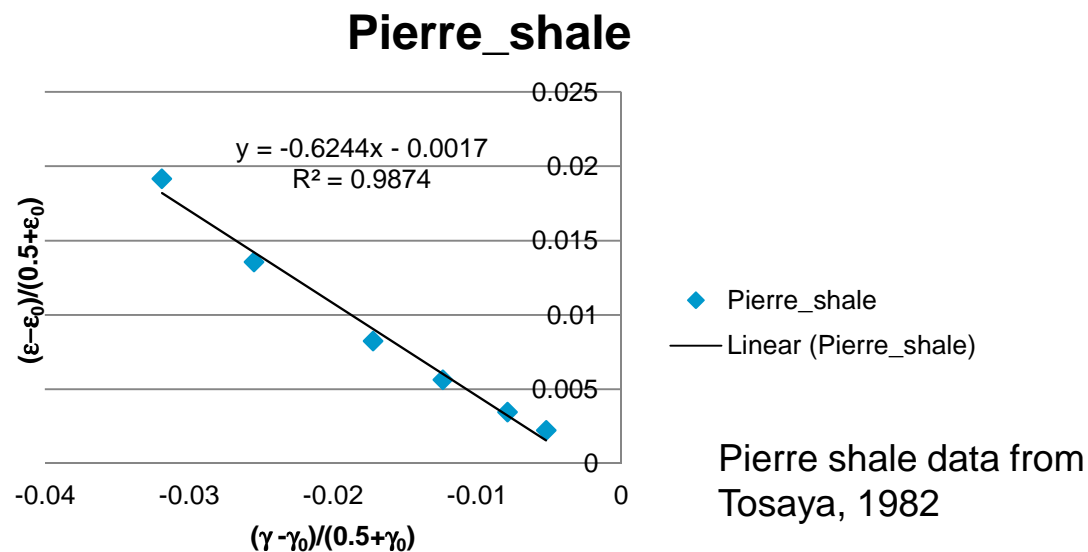


Assume that  $D$  is actually quasi-static and has an associated Debye-type time constant,

$$D \propto \frac{1}{1 + \omega^2 \tau^2}$$

For the Norwegian Sea shale,  $D = 0,63$ . This gives  $\tau = 1,2 \cdot 10^{-7}$  s at 1 MHz which is in the range of the stress-response time constants obtained from the GSLS fits to the spectral data for this shale ( $1,6 \cdot 10^{-7}$  s to  $1,13 \cdot 10^{-7}$  s).

# Time constant implications



For the Pierre shale,  $\text{abs}(D) = 0,278$ . This gives  $\tau = 2,57 \times 10^{-7}$  s at 1 MHz which is in the range of the stress-response time constants obtained from the GSLS fits ( $2,86 \times 10^{-7}$  s to  $2,34 \times 10^{-7}$  s) to the spectral data. The significance of the minus sign is yet to be explained.



# Conclusions

- The spectral ratio method for attenuation measurements can yield some of the frequency dependence of the shale attenuation,  $1/Q$  provided the transducer bandwidth is wide enough.
- The frequency dependence of attenuation at ultrasonic frequencies was a good fit to the GSLS model yielding two time constants. The first constant is a stress-response time and the second is related to strain relaxation. Only the first constant is considered here.
- A time constant obtained from the Budiansky-O'Connell drainage parameter,  $D$ , assuming Debye relaxation for a fluid-saturated cracked solid, agreed closely with the GSLS parameters associated with the stress response-time of the shales.
- This implies that fluid-filled cracks play a role in the stress response times and the changing anisotropy of the shales as confining and pore pressures varies.

**CSIRO CESRE & SINTEF FORMATION  
PHYSICS**

Anthony Siggins

Phone: +613 9545 8359

Email: [tony.siggins@csiro.au](mailto:tony.siggins@csiro.au)

Web: [www.csiro.au](http://www.csiro.au)

[www.csiro.au](http://www.csiro.au)

Thank you

**Contact**

Phone: 1300 363 400 or +61 3 9545 8359

Email: [enquiries@csiro.au](mailto:enquiries@csiro.au) Web: [www.csiro.au](http://www.csiro.au)

